

QCD CORRECTIONS TO HIGGS BOSON DECAYING INTO BOTTOM QUARKS*

WOJCIECH BIZOŃ

Institut für Theoretische Teilchenphysik (TTP), KIT, 76128 Karlsruhe, Germany
and

Institut für Kernphysik (IKP), KIT, 76344 Eggenstein-Leopoldshafen, Germany

(Received May 5, 2020)

The largest decay channel of the Higgs boson is to bottom quarks. In these proceedings, we describe tools that facilitate high-precision simulation of the $H \rightarrow b\bar{b}$ decay. We present an event generator, constructed using the MinLO method, which allows us to consistently match the next-to-next-to-leading order (NNLO) QCD corrections to Higgs boson decaying into massless b quarks with a parton shower (PS). Furthermore, we present an NNLO QCD calculation of the Higgs boson decay into b quarks with full treatment of the b -quark mass. These calculations provide a state-of-the-art description of the $H \rightarrow b\bar{b}$ decay and, therefore, they will be important for studying the Higgs boson itself.

DOI:10.5506/APhysPolB.51.1287

1. Introduction

The discovery of the Higgs boson, by ATLAS and CMS collaborations in 2012, has, not only, formally completed the Standard Model (SM) but also opened a new window for studying particle physics by exploring properties of the newly discovered boson. Since the Higgs boson's mass has already been accurately measured [1], all couplings between the SM particles and the Higgs boson can be predicted. Nevertheless, these couplings can be altered by phenomena that are not captured by the SM and require its extension. Therefore, measuring the actual size of couplings in the Higgs sector can provide clues and constraints on many possible extensions of the SM.

One of the most interesting processes that can be studied at the Large Hadron Collider (LHC) is the associated Higgs production (VH) process which involves a production of the Higgs boson (H) accompanied by an additional electroweak gauge boson (V) [2]. The $pp \rightarrow VH$ process gives

* Presented at XXVI Cracow Epiphany Conference on LHC Physics: Standard Model and Beyond, Kraków, Poland, January 7–10, 2020.

a unique access to the VVH couplings which are completely fixed by the symmetries of the SM but might be modified by New Physics phenomena. Furthermore, studying the VH production, in combination with the $H \rightarrow b\bar{b}$ decay, allows for a direct measurement of the b -quark Yukawa coupling.

The Higgs boson decay into a pair of bottom quarks, $H \rightarrow b\bar{b}$, is the most common decay channel of the Higgs boson and, therefore, it is often the channel to consider when studying associated Higgs production [3, 4]. Nevertheless, since b quarks are coloured partons, they cannot be directly observed in the detectors, instead, they need to be studied by using jets. Although this kind of measurements are very challenging, due to overwhelming QCD backgrounds, many sophisticated techniques have been developed to improve efficiency of the VH signal extraction [5].

In order to fully utilise the wealth of data coming from the LHC, a good theoretical understanding of the $H \rightarrow b\bar{b}$ process is essential. This subject has been already extensively studied in the past [6–10] with fully-differential next-to-next-to-leading order (NNLO) QCD calculations providing the state-of-the-art predictions and first N³LO results appearing [11]. Furthermore, a transition from a limited multiplicity of final states, as described by fixed-order calculations, to a realistic picture of events with $\mathcal{O}(100)$ particles can be achieved by using parton-shower algorithms to simulate additional radiation. In the context of associated Higgs production, such effects have been explored [12–18].

Building on this ground, we present a matching of NNLO fixed-order corrections with PS that was obtained in Ref. [17]. Moreover, we present efforts undertaken to study the b -quark mass effects on the $H \rightarrow b\bar{b}$ decay contained in Ref. [19].

2. NNLO+PS matching using MiNLO method

In this section, we present an event generator that was described in Ref. [17]. It facilitates simulation of the $H \rightarrow b\bar{b}$ decay at NNLO QCD with further PS effects. Such a construction is achieved by merging the $H \rightarrow b\bar{b}$ and $H \rightarrow b\bar{b}g$ generators using the MiNLO method [20] and then performing an NNLO reweighting. This calculation was performed with massless b quarks which, given the large operating energy of the LHC and smallness of b -quark mass with respect to the Higgs boson mass, is often a good approximation.

2.1. Merging of $H \rightarrow b\bar{b}$ and $H \rightarrow b\bar{b}g$ generators

We consider the decay of the Higgs boson into a pair of massless bottom quarks accompanied by an additional gluon

$$H(p_1) \rightarrow b(q_1) + \bar{b}(q_2) + g(q_3). \quad (1)$$

The usual MiNLO procedure [20, 21] enables us to combine the $H \rightarrow b\bar{b}$ and $H \rightarrow b\bar{b}g$ event generators into a single one, without introducing an auxiliary merging scale. This is accomplished by combining an NLO fixed-order calculation of the $H \rightarrow b\bar{b}g$ decay together with information encoded in the Sudakov form factor of a next-to-next-to-leading-logarithmic (NNLL) resummed prediction for the three-jet resolution parameter y_3 [22, 23]. We define the jet resolution with the Cambridge algorithm [24, 25].

The merged event generator is constructed within the POWHEG-BOX-V2 framework. The usual POWHEG \bar{B} function [26], upgraded with the MiNLO method reads

$$\bar{B}(\Phi_{b\bar{b}g}) = \alpha_s(q_t^2) \Delta^2(y_3) \left[B_{b\bar{b}g} \left(1 - 2\Delta^{(1)}(y_3) \right) + V_{b\bar{b}g} + \int d\Phi_r R_{b\bar{b}g} \right], \tag{2}$$

where the $\Phi_{b\bar{b}g}$ is the phase space of the three-body $H \rightarrow b\bar{b}g$ decay; the Sudakov form factor is denoted by $\Delta(y_3)$, and $\Delta^{(1)}(y_3)$ stands for its $\mathcal{O}(\alpha_s)$ expansion. Symbols $B_{b\bar{b}g}$, $V_{b\bar{b}g}$ and $R_{b\bar{b}g}$ represent the Born, virtual and real amplitudes, respectively. The virtual and real amplitudes as well as the $\Delta^{(1)}(y_3)$ factor contain an additional power of the strong coupling α_s which is also evaluated at $q_t^2 = y_3 M_H^2$.

The MiNLO method ensures that we obtain NLO accurate description of $H \rightarrow b\bar{b}$ observables simply by integrating over the radiation phase space. In this case, we retain the NLO partial decay width $\Gamma_{H \rightarrow b\bar{b}}$, *i.e.*

$$\Gamma_{H \rightarrow b\bar{b}}^{\text{MiNLO}} \equiv \frac{1}{2M_H} \int d\Phi_{b\bar{b}g} \bar{B}(\Phi_{b\bar{b}g}) = \Gamma_{H \rightarrow b\bar{b}}^{\text{NLO}} + \mathcal{O}(\alpha_s^2). \tag{3}$$

Such a statement can be verified numerically by taking the $\alpha_s \rightarrow 0$ limit and calculating the difference between $\Gamma_{H \rightarrow b\bar{b}}^{\text{MiNLO}}$ and an analytical prediction for $\Gamma_{H \rightarrow b\bar{b}}^{\text{NLO}}$,

$$\delta(\alpha_s) = \frac{1}{\alpha_s^2} \frac{\Gamma_{H \rightarrow b\bar{b}}^{\text{MiNLO}} - \Gamma_{H \rightarrow b\bar{b}}^{\text{NLO}}}{\Gamma_{H \rightarrow b\bar{b}}^{\text{LO}}}. \tag{4}$$

We performed such a test and we report its results in Fig. 1. We studied the behaviour of $\delta(\alpha_s)$, defined in Eq. (4), as a function of the strong coupling α_s . In case spurious $\mathcal{O}(\alpha_s^{3/2})$ terms were present in the $\Gamma_{H \rightarrow b\bar{b}}^{\text{MiNLO}}$ result, the difference $\delta(\alpha_s)$ would feature an increasing behaviour when approaching the small α_s limit. Conversely, we see that the curves depicted in Fig. 1 flatten out as approaching $\alpha_s \rightarrow 0$ confirming the claim of Eq. (3).

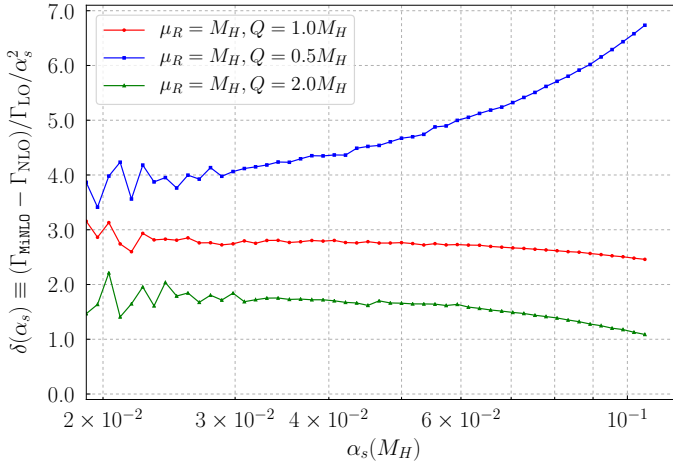


Fig. 1. Numerical check of the NLO accuracy of the MiNLO method. The fact that $\delta(\alpha_s)$ approaches a constant at small α_s , rather than increasing as $1/\sqrt{\alpha_s}$, shows that $\mathcal{O}(\alpha_s)$ terms in Γ_{MiNLO} and Γ_{NLO} agree and that no spurious $\alpha_s^{3/2}$ terms are present in the Γ_{MiNLO} result. The renormalisation scale was set to $\mu_R = M_H$. We tested three different resummation scales Q .

The events generated using the above procedure are further reweighted to match the NNLO partial decay width $\Gamma_{H \rightarrow b\bar{b}}^{\text{NNLO}}$. To this end, the weight of each event is rescaled by a factor

$$\mathcal{W} = \frac{\Gamma_{H \rightarrow b\bar{b}}^{\text{NNLO}}}{\Gamma_{H \rightarrow b\bar{b}}^{\text{MiNLO}}}. \quad (5)$$

Note that, in general, the reweighting factor is a function of the phase space of the underlying process. Nevertheless, the $H \rightarrow b\bar{b}$ decay is isotropic due to the scalar nature of the Higgs boson and hence the reweighting factor reduces to a constant. Some variations in the NNLO reweighting procedure are allowed, *cf.* [17, 20].

2.2. Matching to a parton shower

Since the Higgs boson is a scalar particle, the $H \rightarrow b\bar{b}$ events generated according to the procedure described in Section 2.1 can be easily interfaced with any Higgs boson production events.

The combination of production (`event_Hprod`) and decay (`event_Hdec`) events boils down to taking all momenta of the Higgs decay products, boosting them such that their total momentum matches the momentum of a Higgs boson in the production event and recombining the two events into one. Weights of the resulting event are constructed by multiplying the weights of `event_Hprod` and `event_Hdec`.

Note that, in POWHEG-BOX-V2 framework, events are equipped with a `scalup` variable that sets an upper bound for radiation which has to be respected during the PS evolution. The amalgamated event contains the upper bound of the production event, `scalup_prod`, while the bound for radiation in the decay part, `scalup_dec`, can be reconstructed using kinematics and colour connections registered in the event entries of the decay products.

In order to ensure consistency of fixed-order calculation and PS evolution, we pass the production bound, `scalup_prod`, to the shower program, *e.g.* PYTHIA 8 [27]. For constraining the radiation emitted off the decay products, we construct a vetoed shower, *i.e.* using `Pythia8` we generate emissions off the decay products in the whole available phase space and, after the shower is completed, check the hardness of the splittings that were generated. In case splittings harder than those allowed by the `scalup_dec` are present, we reject the shower history and repeat the evolution once again. This procedure is repeated until all splittings respect the `scalup_dec` bound.

2.3. Applications

This simple method allows us to describe $H \rightarrow b\bar{b}$ decay with a state-of-the-art NNLO accuracy matched to a parton shower. As a proof of principle, we used it to describe associated Higgs production and vector boson fusion (VBF) processes, see Ref. [17]. The method can be easily applied to any other Higgs production process, provided the events are generated within the POWHEG-BOX-V2 framework.

3. NNLO with massive b quarks

In this section, we present an NNLO QCD calculation of the $H \rightarrow b\bar{b}$ decay with a complete treatment of the bottom-quark mass. This problem is not only interesting in its own right, but is also a step towards studying b -quark mass effects in, for example, associated Higgs production.

Despite the fact that the b -quark mass is small in comparison with the Higgs boson mass, there are a few reasons that make it interesting to explore the mass effects in the $H \rightarrow b\bar{b}$ decay. On the one hand, the phase space of the Higgs decay is large and there are regions where sensitivity to the b -quark mass is enhanced due to the presence of energy scales which are not very different of the b -quark mass. Furthermore, studying b -quarks involves clustering algorithms which are used to identify jets. For massless b quarks, one needs to resort to flavoured jet algorithms [28], while a computation involving massive b quarks allows us to use conventional jet algorithms, such as the anti- k_t [29], and make the theoretical predictions and experimental analyses more aligned. Finally, there are particular contributions, *cf.* Fig. 2,

involving a Higgs boson decaying to b quarks which are mediated by a top-quark loop [8, 30]. They cannot be incorporated into a fully-differential massless calculation. In what follows, we refer this contribution as the $y_b y_t$ contribution. Altogether, it is important to consider and explore such effects when providing high-precision predictions for the $H \rightarrow b\bar{b}$ decay.

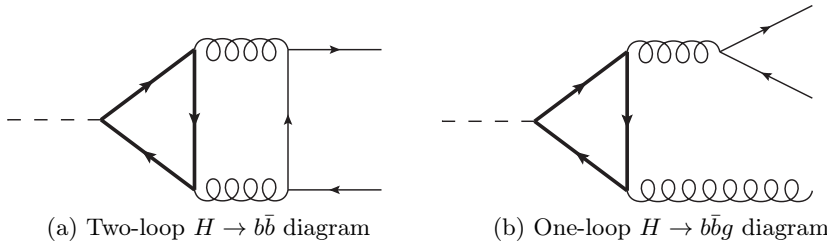


Fig. 2. The top-Yukawa contributions to the $H \rightarrow b\bar{b}$ and $H \rightarrow b\bar{b}g$ amplitudes. The solid thick lines represent a top quark, while the thin solid lines denote the external bottom quarks.

Here, we work in the nested soft-collinear subtraction scheme [31–33] that relies on the sector-improved residue subtraction [34–37]. We include the b -quark mass effects according to treatment outlined in Ref. [36].

3.1. Overview

One of the challenges in higher-order QCD calculations is the treatment of infrared singularities. These arise when massless particles become soft or collinear and, within dimensional regularisation, they are manifested as poles in the regularisation parameter $\epsilon = (4 - d)/2$. When considering infrared observables, the $1/\epsilon$ poles cancel out between the real and virtual corrections. Nevertheless, the observables depend on momenta of the real emissions and, since observables are often non-trivial due to complicated kinematic constraints or jet algorithms, the numerical phase-space integration is a desirable feature. This can be achieved, for example, by using a subtraction scheme to regulate the singular limits of the phase space and render them integrable.

For an integral of a function F , we schematically write

$$\langle F \rangle = \langle F - OF \rangle + \langle OF \rangle, \quad (6)$$

where $\langle \dots \rangle$ denotes the phase-space integration and O is an operator which extracts the asymptotic behaviour of function F in a singular limit. The term $\langle OF \rangle$ is integrated over the d -dimensional unresolved phase space, *i.e.* the phase space of soft and collinear real emissions. For this reason this term contains explicit $1/\epsilon$ poles which are then cancelled against the ones present

in the virtual corrections. On the other hand, the regulated term $\langle F - OF \rangle$ is integrated numerically in four dimensions. Such a procedure is applied recursively to all singular limits.

Within the nested soft–collinear subtraction scheme, one starts by introducing subtraction terms in the soft limits, which at NNLO involves up to two single-soft limits and the double-soft limit. This is followed by partitioning the phase space such that the collinear limits are isolated and each of them can be suitably parametrised in terms of angles and energies of the partons that can become collinear. Finally, one maps all singularities to the boundaries of the region of integration so that they can be easily extracted by using Eq. (6). The limits of QCD amplitudes in soft and collinear limits can be generated by using the standard QCD factorisation formulae which can be found, for example, in Ref. [36].

This construction allows us to split the calculation into pieces so that the cancellation of $1/\epsilon$ poles, between real and virtual contributions, can be shown without resorting to explicit form of amplitudes.

3.2. The $H \rightarrow b\bar{b}$ process

The $H \rightarrow b\bar{b}$ process is particularly simple since there are no collinear singularities involving b quarks. Moreover, a suitable phase-space parametrisation of the double-real contribution yields only one single-collinear sector.

The NNLO QCD corrections to the $H \rightarrow b\bar{b}$ decay process require several contributions to be considered, *i.e.*

- the double-real contribution (RR) which involves $H \rightarrow b\bar{b}gg$, $H \rightarrow b\bar{b}q\bar{q}$ and $H \rightarrow b\bar{b}b\bar{b}$ subprocesses;
- the real–virtual contribution (RV) which treats one-loop corrections to the $H \rightarrow b\bar{b}g$ process;
- the double-virtual contribution (VV) which entails two-loop corrections to the Born process.

Note that, due to the non-zero b -quark mass, the $H \rightarrow b\bar{b}b\bar{b}$ subprocess is free of infrared singularities and can be calculated directly by integrating the tree-level amplitude over its phase space. All other contributions are divergent in four dimensions, due to the soft and collinear singularities, and require the treatment outlined above.

The double-virtual contribution is calculated using a heavy-quark form factor computed in Ref. [38]. The contribution related to two-loop diagram depicted in Fig. 2 (a) is included using the result of Ref. [39] and subtracting the integrated contribution of the diagram in Fig. 2 (b).

The real–virtual amplitude is obtained using the standard techniques of Passarino–Veltman reduction and spinor-helicity techniques. In the case of the $H \rightarrow b\bar{b}g$ decay, the single-soft divergence of the additional gluon needs to be regulated. We construct a subtraction term using factorisation formula of one-loop amplitudes with massive partons studied in Refs. [40, 41]. The integrated subtraction term is obtained analytically and was presented in Ref. [19].

Finally, to discuss the double-real contribution, we introduce a shorthand notation for the integrand

$$F_{\text{LM}}(b\bar{b}X) = d\Phi_{b\bar{b}X} \left| \mathcal{M}_{b\bar{b}X}^{(0)} \right|^2 \mathcal{F}_{\text{kin}}(b\bar{b}X), \quad (7)$$

where $d\Phi_{b\bar{b}X}$ is the Lorentz invariant phase-space measure of the $H \rightarrow b\bar{b}X$ decay, $|\mathcal{M}_{b\bar{b}X}^{(0)}|^2$ denotes the tree-level squared amplitude and $\mathcal{F}_{\text{kin}}(b\bar{b}X)$ stands for a measurement function of a generic infrared safe observable. We regulate all singular limits of the double-real using the nested soft–collinear subtractions. We start with a subtraction of the double-soft limit, *i.e.* we write

$$\langle F_{\text{LM}}(b\bar{b}gg) \rangle = \langle (I - S_{45})F_{\text{LM}}(b\bar{b}gg) \rangle + \langle S_{45}F_{\text{LM}}(b\bar{b}gg) \rangle, \quad (8)$$

where S_{45} is the operator that extracts the asymptotic behaviour of the $F_{\text{LM}}(b\bar{b}gg)$ term in the double-soft limit. The integrated double-soft term was obtained numerically, *cf.* Ref. [19]. The regulated term requires further subtractions in the collinear limit, where the angle between the momenta of the two gluons vanishes, and in the single-soft limit, where one of the gluons becomes soft. The integrated subtraction terms for these limits coincide with those of a usual NLO calculation and can be found in the literature [42].

Upon combining all contributions, we show cancellation of all $1/\epsilon$ poles without referring to explicit form of matrix elements, *cf.* Sec. 4.4 of Ref. [19]. This cancellation is analytical, except for the double-unresolved contribution where the integrated double-soft subtraction term was calculated numerically.

3.3. Results

We express the $H \rightarrow b\bar{b}$ decay width as a perturbative series in the strong coupling α_s , *i.e.*

$$\Gamma_{H \rightarrow b\bar{b}} = \frac{3}{16\pi} \bar{y}_b^2 M_H \beta^3 \left[1 + \left(\frac{\alpha_s}{\pi} \right) \bar{\gamma}_1 + \left(\frac{\alpha_s}{\pi} \right)^2 \bar{\gamma}_2 \right], \quad (9)$$

where \bar{y}_b is the bottom-quark Yukawa coupling in the $\overline{\text{MS}}$ scheme, $\beta = \sqrt{1 - 4m_b^2/M_H^2}$ with m_b and M_H being the bottom-quark and the Higgs-boson masses. The coefficients $\bar{\gamma}_1$ and $\bar{\gamma}_2$ encode the NLO and NNLO corrections to the decay width.

We present the results in Table I. We used $m_b = 4.78$ GeV as the on-shell bottom-quark mass and $M_H = 125.09$ GeV as the Higgs-boson mass.

Predictions in Table I show a reasonably good perturbative convergence of the $H \rightarrow b\bar{b}$ decay width. The NNLO results are contained within the NLO uncertainty band, which was calculated by varying the renormalisation scale by a factor of two. The correction related to the top-quark mediated decay, *cf.* Fig. 2, increases the NNLO decay width by about 1.7% and a major part of this correction comes from the real-virtual diagram.

TABLE I

The results for the LO, NLO and NNLO $H \rightarrow b\bar{b}$ decay width. The decay width is calculated using our results for the expansion coefficients, $\bar{\gamma}_1$ and $\bar{\gamma}_2$. The uncertainties quoted for the results correspond to numerical integration errors.

μ_R [MeV]	$\frac{1}{2}M_H$	M_H	$2M_H$
$\bar{\Gamma}_{\text{LO}}^{b\bar{b}}$	+2.17005	+1.92702	+1.73274
$\bar{\Gamma}_{\text{NLO}}^{b\bar{b}}$	+2.43161	+2.32781	+2.21731
$\bar{\Gamma}_{\text{NNLO}}^{b\bar{b}}$ (w/o $y_b y_t$)	+2.42041(1)	+2.40333(1)	+2.36344(1)
$\bar{\Gamma}_{\text{NNLO}}^{b\bar{b}}$ (with $y_b y_t$)	+2.44441(1)	+2.42059(1)	+2.37628(1)

4. Conclusions

In these proceedings, we presented new tools that will help with precision studies of the $H \rightarrow b\bar{b}$ decay. Working in the POWHEG-BOX-V2 framework and using the MiNLO method, we constructed an event generator to simulate the $H \rightarrow b\bar{b}$ decay at NNLO QCD accuracy and match these predictions to a parton shower. Such a generator may be used with any Higgs production channel. This calculation has been performed in the limit of massless b quarks, nevertheless, studying mass effects is an important part of the precision programme explored at the LHC. To this end, we prepared an NNLO accurate calculation of the $H \rightarrow b\bar{b}$ decay process with a complete treatment of the b -quark mass. This calculation will also be used for studies of the $H \rightarrow b\bar{b}$ decay with various Higgs production processes. It is desirable to match the massive $H \rightarrow b\bar{b}$ calculation to a parton shower, which we leave for the future work.

I would like to thank the organisers of Epiphany 2020 Conference for a well-organised conference with many stimulating discussions during plenary sessions as well as outside.

REFERENCES

- [1] ATLAS Collaboration, CMS Collaboration (G. Aad *et al.*), *Phys. Rev. Lett.* **114**, 191803 (2015), [arXiv:1503.07589 \[hep-ex\]](#).
- [2] CMS Collaboration (S. Chatrchyan *et al.*), *Phys. Rev. D* **89**, 012003 (2014), [arXiv:1310.3687 \[hep-ex\]](#).
- [3] ATLAS Collaboration (M. Aaboud *et al.*), *Phys. Lett. B* **786**, 59 (2018), [arXiv:1808.08238 \[hep-ex\]](#).
- [4] CMS Collaboration (A.M. Sirunyan *et al.*), *Phys. Rev. Lett.* **121**, 121801 (2018), [arXiv:1808.08242 \[hep-ex\]](#).
- [5] J.M. Butterworth, A.R. Davison, M. Rubin, G.P. Salam, *Phys. Rev. Lett.* **100**, 242001 (2008), [arXiv:0802.2470 \[hep-ph\]](#).
- [6] C. Anastasiou, F. Herzog, A. Lazopoulos, *J. High Energy Phys.* **1203**, 035 (2012), [arXiv:1110.2368 \[hep-ph\]](#).
- [7] V. Del Duca *et al.*, *J. High Energy Phys.* **1504**, 036 (2015), [arXiv:1501.07226 \[hep-ph\]](#).
- [8] F. Caola, G. Luisoni, K. Melnikov, R. Rötsch, *Phys. Rev. D* **97**, 074022 (2018), [arXiv:1712.06954 \[hep-ph\]](#).
- [9] W. Bernreuther, L. Chen, Z.-G. Si, *J. High Energy Phys.* **1807**, 159 (2018), [arXiv:1805.06658 \[hep-ph\]](#).
- [10] R. Gauld *et al.*, *J. High Energy Phys.* **1910**, 002 (2019), [arXiv:1907.05836 \[hep-ph\]](#).
- [11] R. Mondini, M. Schiavi, C. Williams, *J. High Energy Phys.* **1906**, 079 (2019), [arXiv:1904.08960 \[hep-ph\]](#).
- [12] S. Frixione, B.R. Webber, [arXiv:hep-ph/0506182](#).
- [13] K. Hamilton, P. Richardson, J. Tully, *J. High Energy Phys.* **0904**, 116 (2009), [arXiv:0903.4345 \[hep-ph\]](#).
- [14] F. Granata, J.M. Lindert, C. Oleari, S. Pozzorini, *J. High Energy Phys.* **1709**, 012 (2017), [arXiv:1706.03522 \[hep-ph\]](#).
- [15] G. Luisoni, P. Nason, C. Oleari, F. Tramontano, *J. High Energy Phys.* **1310**, 083 (2013), [arXiv:1306.2542 \[hep-ph\]](#).
- [16] W. Astill, W. Bizoń, E. Re, G. Zanderighi, *J. High Energy Phys.* **1811**, 157 (2018), [arXiv:1804.08141 \[hep-ph\]](#).
- [17] W. Bizoń, E. Re, G. Zanderighi, [arXiv:1912.09982 \[hep-ph\]](#).
- [18] S. Alioli *et al.*, *Phys. Rev. D* **100**, 096016 (2019), [arXiv:1909.02026 \[hep-ph\]](#).
- [19] A. Behring, W. Bizoń, *J. High Energy Phys.* **2001**, 189 (2020), [arXiv:1911.11524 \[hep-ph\]](#).

- [20] K. Hamilton, P. Nason, C. Oleari, G. Zanderighi, *J. High Energy Phys.* **1305**, 082 (2013), [arXiv:1212.4504 \[hep-ph\]](#).
- [21] K. Hamilton, P. Nason, G. Zanderighi, *J. High Energy Phys.* **1210**, 155 (2012), [arXiv:1206.3572 \[hep-ph\]](#).
- [22] A. Banfi, H. McAslan, P.F. Monni, G. Zanderighi, *Phys. Rev. Lett.* **117**, 172001 (2016), [arXiv:1607.03111 \[hep-ph\]](#).
- [23] A. Banfi, H. McAslan, P.F. Monni, G. Zanderighi, *J. High Energy Phys.* **1505**, 102 (2015), [arXiv:1412.2126 \[hep-ph\]](#).
- [24] Y.L. Dokshitzer, G.D. Leder, S. Moretti, B.R. Webber, *J. High Energy Phys.* **9708**, 001 (1997), [arXiv:hep-ph/9707323](#).
- [25] S. Bentvelsen, I. Meyer, *Eur. Phys. J. C* **4**, 623 (1998), [arXiv:hep-ph/9803322](#).
- [26] S. Frixione, P. Nason, C. Oleari, *J. High Energy Phys.* **0711**, 070 (2007), [arXiv:0709.2092 \[hep-ph\]](#).
- [27] T. Sjöstrand, S. Mrenna, P.Z. Skands, *Comput. Phys. Commun.* **178**, 852 (2008), [arXiv:0710.3820 \[hep-ph\]](#).
- [28] A. Banfi, G.P. Salam, G. Zanderighi, *Eur. Phys. J. C* **47**, 113 (2006), [arXiv:hep-ph/0601139](#).
- [29] M. Cacciari, G.P. Salam, G. Soyez, *J. High Energy Phys.* **0804**, 063 (2008), [arXiv:0802.1189 \[hep-ph\]](#).
- [30] A. Primo, G. Sasso, G. Somogyi, F. Tramontano, *Phys. Rev. D* **99**, 054013 (2019), [arXiv:1812.07811 \[hep-ph\]](#).
- [31] F. Caola, K. Melnikov, R. Röntsch, *Eur. Phys. J. C* **77**, 248 (2017), [arXiv:1702.01352 \[hep-ph\]](#).
- [32] F. Caola, K. Melnikov, R. Röntsch, *Eur. Phys. J. C* **79**, 386 (2019), [arXiv:1902.02081 \[hep-ph\]](#).
- [33] F. Caola, K. Melnikov, R. Röntsch, *Eur. Phys. J. C* **79**, 1013 (2019), [arXiv:1907.05398 \[hep-ph\]](#).
- [34] M. Czakon, *Phys. Lett. B* **693**, 259 (2010), [arXiv:1005.0274 \[hep-ph\]](#).
- [35] M. Czakon, *Nucl. Phys. B* **849**, 250 (2011), [arXiv:1101.0642 \[hep-ph\]](#).
- [36] M. Czakon, D. Heymes, *Nucl. Phys. B* **890**, 152 (2014), [arXiv:1408.2500 \[hep-ph\]](#).
- [37] M. Czakon, A. van Hameren, A. Mitov, R. Poncelet, *J. High Energy Phys.* **1910**, 262 (2019), [arXiv:1907.12911 \[hep-ph\]](#).
- [38] J. Ablinger *et al.*, *Phys. Rev. D* **97**, 094022 (2018), [arXiv:1712.09889 \[hep-ph\]](#).
- [39] S.A. Larin, T. van Ritbergen, J.A.M. Vermaseren, *Phys. Lett. B* **362**, 134 (1995), [arXiv:hep-ph/9506465](#).
- [40] A. Mitov, S. Moch, *J. High Energy Phys.* **0705**, 001 (2007), [arXiv:hep-ph/0612149](#).
- [41] I. Bierenbaum, M. Czakon, A. Mitov, *Nucl. Phys. B* **856**, 228 (2012), [arXiv:1107.4384 \[hep-ph\]](#).
- [42] S. Alioli, P. Nason, C. Oleari, E. Re, *J. High Energy Phys.* **1006**, 043 (2010), [arXiv:1002.2581 \[hep-ph\]](#).